

Mechanical characterisation of additively manufactured material having lattice microstructure

This content has been downloaded from IOPscience. Please scroll down to see the full text.

2015 IOP Conf. Ser.: Mater. Sci. Eng. 74 012004

(<http://iopscience.iop.org/1757-899X/74/1/012004>)

View [the table of contents for this issue](#), or go to the [journal homepage](#) for more

Download details:

IP Address: 152.78.0.15

This content was downloaded on 22/10/2015 at 18:26

Please note that [terms and conditions apply](#).

Mechanical characterisation of additively manufactured material having lattice microstructure

E Cuan-Urquizo¹, S Yang² and A Bhaskar¹

¹ Computational Engineering and Design Group, Faculty of Engineering and the Environment, University of Southampton, SO17 1BJ, UK

² Engineering Materials Research Group, Faculty of Engineering and the Environment, University of Southampton, SO17 1BJ, UK

E-mail: E.CuanUrquizo@soton.ac.uk

Abstract. Many natural and engineered structures possess cellular and porous architecture. This paper is focused on the mechanical characterisation of additively manufactured lattice structures. The lattice consists of a stack of polylactic acid (PLA) filaments in a woodpile arrangement fabricated using a fused deposition modelling 3D printer. Some of the most promising applications of this 3D lattice material of this type include scaffolds for tissue engineering and the core for sandwich panels. While there is a significant body of work concerning the manufacture of such lattice materials, attempts to understand their mechanical properties are very limited. This paper brings together manufacturing with the need to understand the structure-property relationship for this class of materials. In order to understand the elastic response of the PLA-based lattice structures obtained from the fused deposition modelling process, single filaments manufactured using the same process were experimentally characterised first. The single PLA filaments were manufactured under different temperatures. These filaments were then characterised by using tensile testing. The stress-strain curves are presented. The variability of the measured results is discussed. The measured properties are then taken as input to a finite element model of the lattice material. This model uses simple one-dimensional elements in conjunction with a novel method achieving computational economy which precludes the use of fine meshes. Using this novel model, the apparent elastic modulus of lattice along the filaments has been obtained and is presented in this paper.

1. Introduction

Many natural structures such as trees and skeletons are made of cellular materials such as bone and wood [1]. Engineers and builders used cellular materials for several centuries such as wood or cork in various applications [1]. However, modern synthetic cellular solids require design, analysis, manufacture and optimisation. An apparent property of this class of materials is the relative density, defined as the density of the cellular solid divided by that of the solid it is made from [2]. When properly architected, the materials show high stiffness to weight ratio [3].

Additive manufacturing has emerged as an option for fabricating cellular materials, since the fabrication of lattices with customised 3D-shapes has been developed [4, 5]. The manufacture process employed in this work is fused deposition modelling (FDM). FDM is a well-known additive manufacturing (AM) process used to produce prototypes and more recently, end use parts [6]. The parts are built by means of extrusion of filaments through nozzle head. The extruder head moves following a specific path on the printing plane (XY plane) then moving



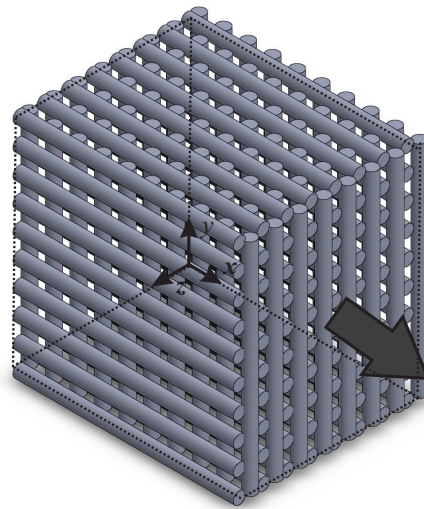


Figure 1. CAD model of the lattice structure.

along the axis perpendicular to the printing plane (Z axis), resulting in a layer by layer manufactured part. Due to the thermal processes taking place during the printing procedure, each layer bonds with the previous layer extruded.

In tissue engineering, scaffolds require optimal biological characteristics to facilitate the proliferation of the cells. They also are required to have mechanical properties sufficient to withstand loading due to the ingrowth of tissue during their use [5, 7]. Initial attempts to understand and predict the mechanical behaviour of this type of lattice structures used as scaffolds for tissue engineering have been presented in [4, 8, 9]. In [4, 8], finite element analysis (FEA) is used to predict the mechanical behaviour of scaffolds fabricated using robocasting and selective laser sintering. The models were meshed using tetrahedral and brick elements respectively. A model to obtain the elastic moduli of the scaffold desired as a function of the diameter of the filaments, spacing and overlap between layers is presented in [9].

The woodpile architecture can also be found in sandwich plate structures used in aerospace where lightweight and specific stiffness are required [10, 11]. In [10, 11], titanium and nickel-based cylinders in woodpile and woven architectures form lattices used as cores in a sandwich plate structures. Experimental tests, compression and shear, have been conducted on titanium composites-based structures [10]. Models to understand the elastic response of woven lattice structures are presented and compared with experimental measurements on stainless steel structures in [11]. From the literature reviewed, it emerges that despite the flurry of activities in the area of additive manufacturing, studies on the mechanics of material thus produces are limited.

The structure of this paper is as follows. In order to characterise the elastic response of the lattice material, single filaments were manufactured via FDM and tested under tensile loads. The measured stress-strain curves are presented in Section 3. The Young's modulus obtained from these curves is then used as input for a novel finite element model to calculate the elastic response of the lattice structure along the filaments direction. The FEA model is presented in Section 4. Finally, conclusions and future work are presented in Section 5.

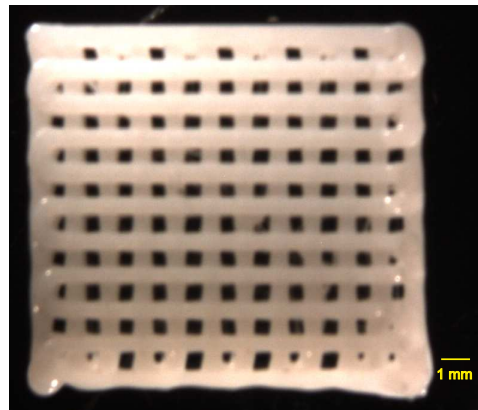


Figure 2. 3D Printed lattice material.

2. Fused deposition modelling as a manufacturing process

As mentioned earlier, the lattice structure of interest within this paper is fabricated using FDM. FDM, as with most other common additive manufacturing techniques, makes use of depositing the material in a semi-molten state. Material in this state is deposited spatially in a manner guided by a set of computer instructions known as G-codes that drive the nozzle. Each layer of the material thus extruded then fuses with the adjacent layers previously deposited. In order to have a complete control on the internal architecture of the material, our approach here is to use a MATLAB code first, which generates the G-codes for the required internal geometry. Using this code it was possible to control the distance between each filament, in the XY plane, the distance between each layer, the number of layers, the number of filaments parallel to the X axis, and parallel to the Y axis. In contrast, standard additive manufacturing techniques rely on the instructions generated by the machine once a CAD-file is provided to the AM machine.

In the past, there have been several studies related to the manufacture of parts using various additive manufacturing processes. The attention of previous authors on porosity control and the properties of components thus manufactured, is limited. Analysis on the mechanical properties of parts manufactured using FDM can be found in [6, 12–17]. However, in these studies, there was no attempt to control the porosity of the manufactured parts.

A final 3D printed lattice is shown in Figure 2. This printed lattice has porosity of 1×1 mm in the printing plane and 10 layers in the axis perpendicular to the printing plane. The same manufacture parameters used to print the lattice were used to print single filaments. These filaments were then submitted to tensile tests. The results are presented in the next section.

3. Single filaments characterisation

The first step towards the characterisation of the lattice structure is to test a single filament having the same cross-section, material and manufacturing conditions (e.g. temperature) as the actual parts. DEBEN MICROTTEST[®] module was used for tensile testing (see Fig. 3). The testing module consists of two clamps that can be brought close to each other up to 10 mm apart. Further extension up to 10 mm can be achieved by a controlled motor with displacement and force sensing transducers. Using the software module, load-extension curves of the single filaments were obtained. The data were imported into MATLAB for further processing. From the displacement and force information provided by the tensile testing machine, stress and strain were calculated after incorporating cross-sectional information and the gauge length of the samples.

The cross-sectional area has been approximated as an ellipse as it appeared reasonable from

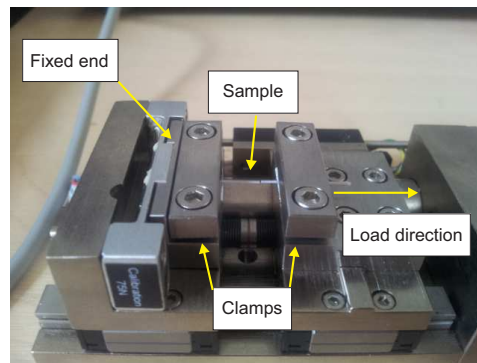


Figure 3. The Deben MICROTTEST [®] module showing the principal components and a single filament. The sample shows failure away from the two clamped ends.

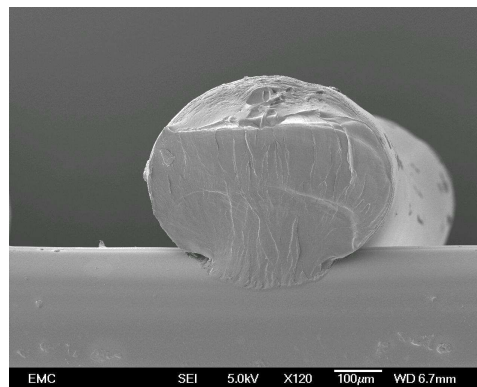


Figure 4. SEM image of the fractural surface showing adhesion with the adjacent layer.

the appearance (Figure 4). The minor and major axes for 10 filaments were measured using a macroscope. The mean area was obtained as $1.8167 \times 10^{-7} \text{m}^2$. This value for the area was later used to obtain the stress for plotting the stress-strain curves.

Single filaments were tested under quasi-static conditions of slow extension rate. After scaling the force and extension values with respect to the cross-sectional area and the original length, stress-strain curves were obtained and are presented in Figures 5, 6 and 7. These results refer to filaments manufactured at 180 °C, 190 °C, and 200 °C respectively.

From these stress-strain curves, the Young's modulus was obtained. The results are presented in Table 1. The Young's modulus is seen to be fairly consistent for all the cases in the range of 3.0 – 3.5 GPa (which is within the range of the value reported in the literature [5]). However, the failure stress shows remarkable variability. This variability could be attributed to several factors. One of the most significant sources of this variability appears to be bubble formed during the melting process. This is expected to introduce variability in strength that is very different from sample to sample. Additionally, factors such as variability in the cross-sectional area, the difficulty in their accurate measurement, inevitable variability at the clamping location, etc. have an effect on the variability. Conducting an experimental error analysis, the formula $\sigma = F/\pi r^2$ for the stress calculation, assuming a perfect circular cross-section resulted in: $|d\sigma/\sigma| = |dF/F| + 2|dr/r|$. Note the factor of 2 that appears with the radius term resulting in *twice* the overall error in the stress calculation. If the cross-section is treated as an ellipse instead,

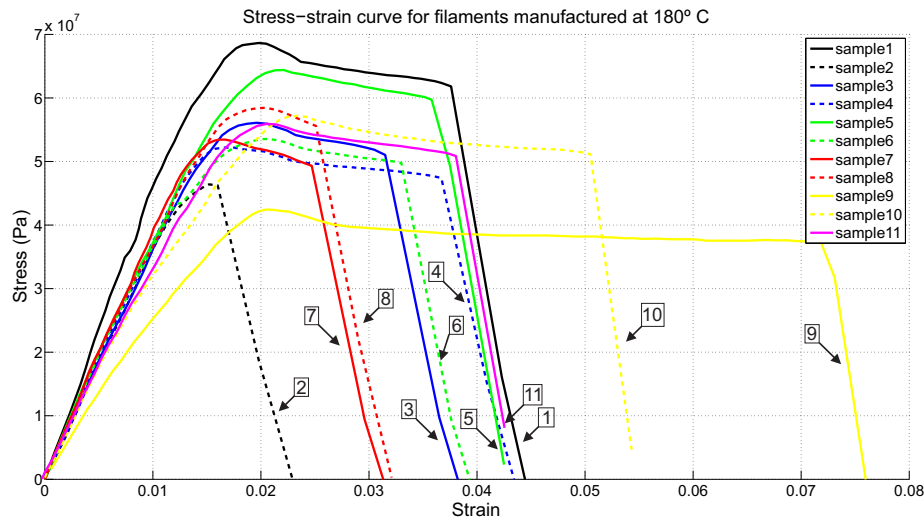


Figure 5. Stress-strain curve for filaments manufactured at 180 °C. For convenience, numerical labels with each curve indicate the sample number.

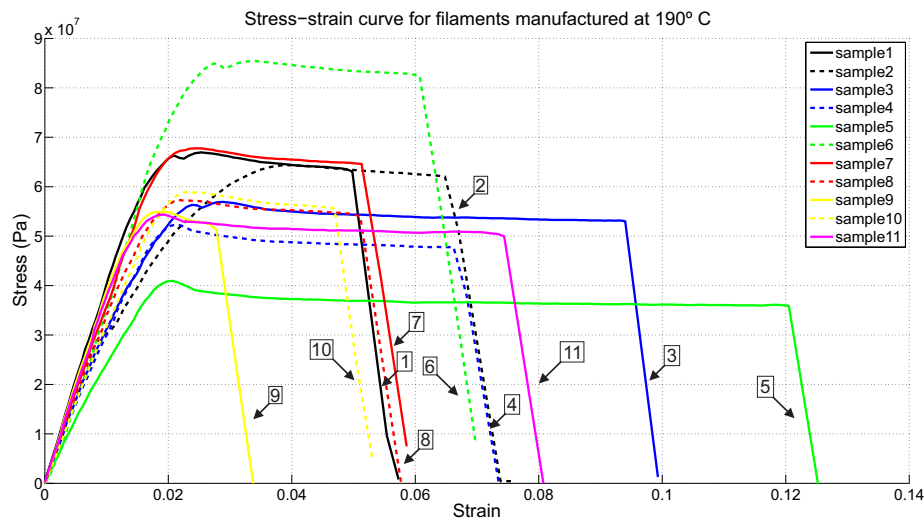


Figure 6. Stress-strain curve for filaments manufactured at 190 °C. For convenience, numerical labels with each curve indicate the sample number.

the formula for stress changes to $\sigma = F/\pi ab$ where a and b are the major and minor radii of the ellipse, we obtain $|d\sigma/\sigma| = |dF/F| + |da/a| + |db/b|$ where the errors in the measurements of the minor and major axis of the ellipse will add up affecting the the final percentage error. This highlights the sensitivity in the measurements of the cross-sectional dimension to the calculated stress. It is envisaged that this may have contributed to the scatter in the modulus of elasticity as observed from different samples. Further study to ascertain this conjecture is under way. The values of the material properties obtained from single-filament tests are subsequently used in the next section for the modelling of the complete lattice.

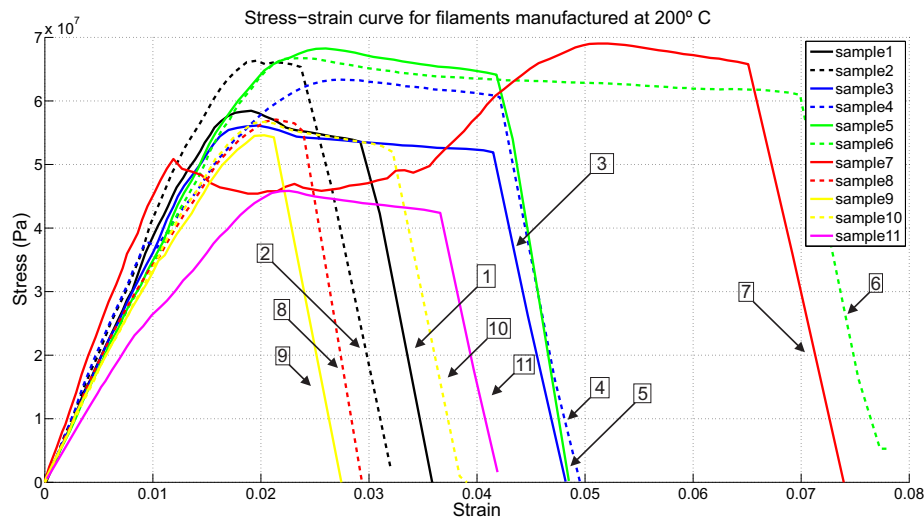


Figure 7. Stress-strain curve for filaments manufactured at 200 °C. For convenience, numerical labels with each curve indicate the sample number.

Table 1. Measured mechanical properties and their variability of single filament samples.

| Temperature (deg) | Young's modulus (GPa) | Std dev. (GPa) | Elongation to break (%) | Std dev. (%) | Yield Strength (MPa) | Std dev. (MPa) |
|----------------------|-----------------------------|-------------------|-------------------------------|-----------------|----------------------------|-------------------|
| 180 | 3.456 | 0.545 | 4.28 | 1.33 | 55.2 | 6.94 |
| 190 | 3.215 | 0.627 | 7.13 | 2.37 | 59.6 | 10.6 |
| 200 | 3.444 | 0.592 | 4.58 | 1.60 | 58.1 | 6.44 |

4. Micromechanical modelling of the complete lattice

In order to understand the apparent elastic response of the lattice material, when the load is applied in one of the directions parallel to the filaments, a finite element model was created. The model employs one-dimensional elements that have stretch and flexure degrees-of-freedom. This leads to computational economy which precludes the use of fine meshes often used by other authors [4, 8]. While a fine mesh is expected to be more accurate, the present analysis is in favour of simple finite elements as one of the purposes of this work is to develop analytical models for such lattice material. Computationally complex models obscure such understanding.

The method consisted on modelling each segment of the filament using Timoshenko beams (*beam188* in ANSYS). Each segment is a part of a filament with FE nodes placed at the physical joints. Figure 8 presents a portion of the lattice structure. The solid lines represent beams that model individual filaments. The dashed lines are the “virtual” elements proposed to simulate the rigidity between each layer. These are necessary because a beam element is a line in space and the non-intersecting filaments on two adjacent planes need to be kept separated by a fixed distance. This distance is equal to the sum of the radii (r_1 and r_2) of the filament belonging to two such layers. Using 3.25 GPa as the material Young's modulus for the model, and 3000 GPa for the virtual element representing the bonding. Several calculations were carried out using

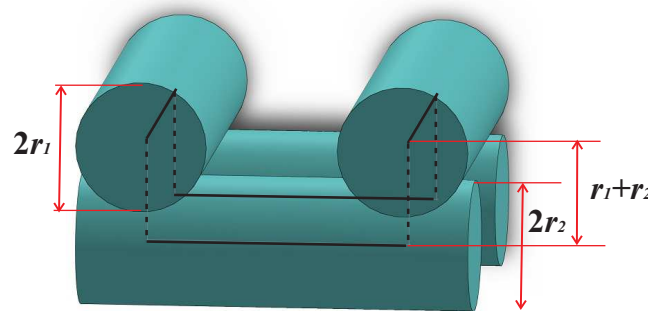


Figure 8. A schematic diagram showing a portion of the lattice structure.

different stiffness values for this virtual element, resulting in negligible differences in the results. This confirms that the virtual elements were stiff enough to be treated as 'rigid'.

The following boundary conditions for the FE simulation were set:

- The nodes lying on the XY plane are constrained to move only in that plane, but not out of it.
- The nodes lying on the YZ plane are constrained to move only in that plane, but no out of it.
- The nodes lying on the XZ plane are constrained to move only in that plane, but no out of it.
- Finally, the origin is constrained in all directions.

The effective elastic modulus along the filaments was obtained as $\bar{E} = 0.596$ GPa. This result is validated using the expected effective modulus relation $\bar{E}_e = E_m \varphi$, where φ is the fractional area $\varphi = aN_f/A$. The fractional area is the relationship between the effective area which is the total area of the single filaments cross-sections (a is the area of a single filament and N_f is the total number of filaments normal to the cross-section of the lattice) and the total area of the lattice cross-section (including air gaps). The expected effective modulus is then $\bar{E}_e = 0.5993$ GPa, which is clearly in agreement with the simple FEA model used here.

5. Conclusions and future work

Mechanical characterisation of lattice material arranged in a woodpile configuration was carried out. Stress-strain curves were measured in the laboratory to characterise single filaments, first. The variability in the elastic response of the filaments, manufactured under nominally identical conditions and carefully tested, was observed. Several reason for this variability, such as, different samples due to manufacture inconsistency, error in measuring the cross-sectional area, and clamping of delicate samples, were identified. For the present study, a nominal cross-sectional area was used to calculate the stresses. In future analyses each sample cross-section will be used for these calculations. The effect of the variability of the measured cross-sectional area in the apparent mechanical property is currently under way. A stochastic model for such lattice material is also being developed.

The effective moduli of the complete lattice along the struts were obtained using a finite element analysis. This was achieved relatively cheaply and effectively by the use of one-dimensional elements in conjunction with 'virtual element' that supposedly are 'rigid'. However the elastic response along the axis perpendicular to the printing plane is significantly more

challenging. Work is in progress in this direction. The bonding between two filaments is likely to play an important role. This aspect of mechanics is currently being studied.

Acknowledgement

This work was supported by the Grants of the Mexican Science and Technology Council (CONACyT) for a PhD degree program at University of Southampton, UK.

References

- [1] Gibson L J and Ashby M F 1999 *Cellular solids: structure and properties* (Cambridge university press)
- [2] Gibson L J 2005 *Journal of Biomechanics* **38** 377–399
- [3] Banerjee S and Bhaskar A 2009 *International Journal of Mechanical Sciences* **51** 598–608
- [4] Miranda P, Pajares A, Saiz E, Tomsia A P and Guiberteau F 2008 *Journal of Biomedical Materials Research Part A* **85** 218–227
- [5] Yang S, Leong K F, Du Z and Chua C K 2001 *Tissue engineering* **7** 679–689
- [6] Bagsik A, Schoppner V and Klemp E 2010 *14th International Scientific Conference on Polymeric Materials*
- [7] Hutmacher D W, Sittinger M and Risbud M V 2004 *TRENDS in Biotechnology* **22** 354–362
- [8] Cahill S, Lohfeld S and McHugh P 2009 *Journal of Materials Science: Materials in Medicine* **20** 1255–1262
- [9] Norato J A and Wagoner Johnson A J 2011 *Journal of biomechanical engineering* **133**
- [10] Moongkhamklang P, Deshpande V S and Wadley H N G 2010 *Acta Materialia* **58** 2822–2835
- [11] Queheillalt D T, Deshpande V S and Wadley H N G 2007 *Journal of Mechanics of Materials and Structures* **2** 1657–75
- [12] Ahn S H, Montero M, Odell D, Roundy S and Wright P K 2002 *Rapid Prototyping Journal* **8** 248–257
- [13] Rodríguez J, Thomas J and Renaud J 2001 *Rapid Prototyping Journal* **7** 148–158
- [14] Magalhaes L, Volpato N and Luersen M 2014 *Journal of the Brazilian Society of Mechanical Sciences and Engineering* **36** 449–459
- [15] Kulkarni P and Dutta D 1999 *Journal of Manufacturing Science and Engineering* **121** 93–103
- [16] Li L, QSun, Bellehumeur C and Gu P 2002 *Journal of Manufacturing Processes* **4** 129–141
- [17] Bellini A and Geri S 2003 *Rapid Prototyping Journal* **9** 252–264